Fluctuation-swamped discontinuous phase changes in lightly doped ferroelectric barium titanate



1992 J. Phys.: Condens. Matter 4 4387

(http://iopscience.iop.org/0953-8984/4/18/006)

J. Phys.: Condens. Matter 4 (1992) 4387–4398. Printed in the UK

# Fluctuation-swamped discontinuous phase changes in lightly doped ferroelectric barium titanate

C N W Darlington† and R J Cernik‡

† School of Physics and Space Research, University of Birmingham, Birmingham B15 2TT, UK

‡ Daresbury Laboratory, Warrington WA4 4AD, UK

Received 17 October 1991, in final form 29 January 1992

**Abstract.** X-ray scattering experiments on lightly doped powders of $BaTiO_3$ using the diffractometer on line 9.1, SRS, Daresbury, have been extended to investigate transitions in the barium-rich solid solutions (Ba,Sr)$TiO_3$ and (Ba,Pb)$TiO_3$. Samples studied earlier were 'impure systems', that is pure material doped with ions with a valency different from those they replaced. Qualitatively the ferroelectric transitions near 130 °C in the solid solutions and impure systems are similar—they are 'smeared out' and appear continuous, but are in fact fluctuation-swamped, discontinuous changes. There are important quantitative differences between the transitions in the two categories. Analysis shows that impure systems behave as 'host'—pure $BaTiO_3$—plus point-like defects, with parameters independent of the dopant and concentration. However, for (Ba,Sr)$TiO_3$ the parameters describing the critical behaviour depend on the concentration of Sr.

## 1. Introduction

The effects of impurities on structural phase transitions in doped and nominally pure systems have received increasing attention in recent years: for example, an EPR study on $BaTiO_3$ doped with $Fe^{3+}$ [1]; the temperature dependence of the Raman spectrum of $KTa_{1-x}Nb_xO_3$ [2]; a study of Raman and hyperRaman scattering in nominally pure $KTaO_3$ [3]; x-ray and neutron scattering experiments on $K(Mn_{1-x}Mg_x)O_3$ [4–6]. The accepted picture is of clusters of the low-temperature phase appearing above the transition temperature, with a (probable) crossover from a displacive to the order–disorder regime as the clusters increase in size with falling temperature [7]. A short review of the extensive French work on lightly doped $BaTiO_3$ has appeared recently [8].

A study of the changes in the shape of x-ray powder diffraction lines with temperature above the ferroelectric transition in $BaTiO_3$ at 130 °C [9] showed that dilute impurities of cerium and niobium, up to 0.3 mol.% produce large fluctuations in the order parameter in both the high- and low-temperature phases; the transition becomes 'smeared out'. Cerium substitutes for barium and niobium substitutes for titanium. The dopants have a valency one higher then the ions they replace and turn the material into an n-type semiconductor [10]. A broadened transition was also found in the as-purchased material; however, after annealing in air at 1200 °C for 30 hours the transition became sharp and discontinuous, with the fluctuations in the order parameter being undetectable.

0953-8984/92/184387+12$04.50  

This paper describes similar x-ray scattering experiments on $Ba(Ti_{0.997}Ta_{0.003})O_3$, $(Ba_{0.997}Sm_{0.003})TiO_3$, three barium-rich compositions in the system (Ba, Sr)$TiO_3$ and $(Ba_{0.99}Pb_{0.01})TiO_3$. $BaTiO_3$ forms solid solutions with both $SrTiO_3$ and $PbTiO_3$ at all compositions. It was anticipated that the solid solutions might behave differently from 'impure systems', that is those with non-isovalent substitutions. The notion of strontium or lead being an impurity in the solid solution is, in any case, inappropriate. Similar changes in lineshape as are reported in [9] were found in all samples studied.

The changes in lineshape are the result of electrostrictive coupling between polarization $P$ and strain $\epsilon$. The line broadening is anisotropic and is caused by a small tetragonal distortion of the high-temperature structure [9]. Taking the polarization to be parallel to [001], then

$$\epsilon_{11} = \epsilon_{22} = Q_{12}P_3^2 \qquad \epsilon_{33} = Q_{11}P_3^2.$$

The change in Bragg angle $\theta$ is given by

$$\Delta(2\theta) = -K[\epsilon_{11}(h^2 + k^2) + \epsilon_{33}l^2]$$

where

$$K = \lambda^2/a^2 \sin(2\theta).$$

## 2. Experimental details

### *2.1. Sample preparation*

The samples were prepared by a standard route. Relevant proportions of 'puratronic' $BaTiO_3$, $SrTiO_3$, $Sm_2O_3$ and $Ta_2O_5$, all obtained from Johnson Matthey Chemicals plc, were mixed together then ball milled under acetone for 30 minutes. The mixtures were held at 1200 °C for 30 hours in a platinum-lined crucible, furnace cooled, then reground.

This procedure could not be adopted for the lead-doped sample because of the volatility of the dopant. First, pure $BaTiO_3$ was annealed at 1200 °C for 30 hours, then ball milled with $PbTiO_3$. The mixture was prereacted at 800 °C for 16 hours, reground and then fired at 1200 °C for 2 hours, following the recipe given in [11].

### *2.2. Diffractometer*

The diffractometer on station 9.1, SRS, Daresbury, UK was used in the high-resolution mode; details are given in [9]. The slit combination gave an angular resolution of about 0.036° in $2\theta$ over most of the angular range studied; the wavelength chosen was 1.0 Å. A rotating flat-plate specimen holder was used because of the high absorption of x-rays by the samples. The furnace was manufactured by GTP Engineering Ltd, and temperature controlled to better than 1 °C using a Newtronic three-term controller.

$\theta$–$2\theta$ step scans through the reflections (110), (111), (200), (211) and (220) were recorded at a number of temperatures above and below the symmetry change. The steps were 0.006° in $2\theta$, and counts were accumulated for two seconds at each point.

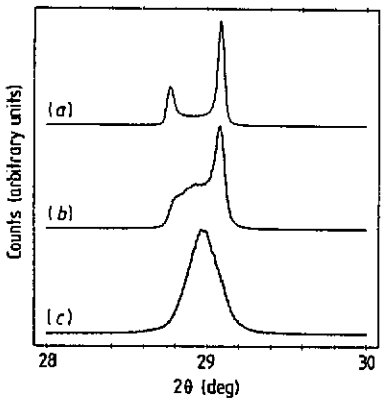


**Figure 1.** Profiles of the (200) reflection from pure $BaTiO_3$ near room temperature: (*a*), annealed at 1200 °C for 30 hours; (*b*), annealed at 1150 °C for 30 hours; (*c*), as-purchased material, annealed at 1000 °C. The peaks have been normalized to have the same peak heights.

## 3. Results

Figure 1 shows the profiles of the (200) reflection at room temperture for the pure material annealed at 1200 °C for 30 hours, at 1150 °C for 30 hours, and the as-purchased powder. Puratronic $BaTiO_3$ is prepared in a vacuum oven at 150 °C, and then annealed at 1000 °C [12], which clearly leaves the material in an inhomogeneously strained state. Chemical analysis showed it to be extremely pure [12].

The scattering between the peaks in figure 1(*a*) was attributed in [9] to inhomogeneous strain caused by 90° domain walls. It is believed that the magnitude of the spontaneous polarization varies in a tanh-like manner in passing from one side of the wall to the other—these walls are about 10–30 unit cells thick [13].

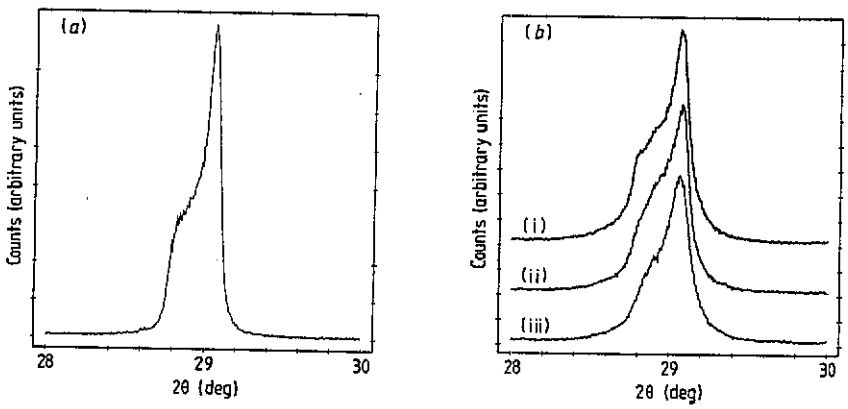


**Figure 2.** Profiles of the (200) reflection near room temperature: (*a*), $Ba(Ti_{0.997}Ta_{0.003})TiO_3$ at 15 °C; (*b*), (Ba, Sr)$TiO_3$ at 20 °C: (i), $(Ba_{0.997}Sr_{0.003})TiO_3$; (ii), $(Ba_{0.99}Sr_{0.01})TiO_3$; (iii), $(Ba_{0.9}Sr_{0.1})TiO_3$.

The effects of doping on (200) at room temperature are shown in figure 2: (*a*), $Ba(Ti_{0.997}Ta_{0.003})O_3$; (*b*), (Ba, Sr)$TiO_3$. Other dopants, such as Sm and Pb, (likewise Ce and Nb [9]), produce similar profiles.

## 4. Analysis

The profiles were fitted with pseudoVoigt functions. The Lorentzian component was typically more than 70% for doped samples above their transition temperature, where the pure sample, annealed at 1200 °C, gave linewidths equal to the resolution of the instrument and a Lorentzian component of about 25%.

### 4.1. Impure systems

*4.1.1. $Ba(Ti_{0.997}Ta_{0.003})O_3$ [Ta (0.003)] and $Ba(Ti_{0.997}Nb_{0.003})O_3$ [Nb (0.003)].* Transition temperatures ($T_t$) were assigned to both samples as the lowest temperature at which the difference plot—the observed profile minus the calculated profile using a single symmetric pseudoVoigt function—was featureless [9]; that is above $T_t$ the line profiles were symmetric, with the average structure possessing cubic symmetry. Values of the transition temperatures for all the samples are given in table 1.

**Table 1.** Values of the transition temperature $T_t$

| Compound | $T_t$ (°C) |
|---|---|
| $BaTiO_3$ | 130 |
| $(Ba_{0.999}Ce_{0.001})TiO_3$ | 126† |
| $(Ba_{0.997}Ce_{0.003})TiO_3$ | 122† |
| $(Ba_{0.997}Sm_{0.003})TiO_3$ | 126 |
| $Ba(Ti_{0.997}Nb_{0.003})O_3$ | 120† |
| $Ba(Ti_{0.997}Ta_{0.003})O_3$ | 122 |
| $(Ba_{0.997}Sr_{0.003}TiO_3$ | 123 |
| $(Ba_{0.99}Sr_{0.01})TiO_3$ | 110 |
| $(Ba_{0.9}Sr_{0.1})TiO_3$ | 100 |
| $(Ba_{0.99}Pb_{0.01})TiO_3$ | 134 |

† From [9]. All other entries, this work.

The FWHM against temperature for Ta (0.003) are shown in figure 3; these diverge as $T - T_t$ decreases. To extract the critical broadening the procedure adopted in [9] was used. Above $T_t$ the lines are essentially Lorentzian, and it was assumed that the total width was the sum of two components; the first owing to instrumental and non-critical sample broadening, the second owing to the critical behaviour. The critical broadening was obtained by subtracting the linewidths at elevated temperature from the widths obtained at lower temperatures. The reflection (111) shows virtually no change in width, because the developing distortion has tetragonal symmetry and, for $BaTiO_3$, $Q_{11} \simeq -2Q_{12}$.

The temperature dependence of the diverging component was fitted to the expression

$$\delta(2\theta) = W(T - T_s)^{-s} \tag{1}$$

where $W$, $T_s$ and $s$ are constants, with $T_s$ set equal to 112 °C. This value makes the log–log plot of (1) linear (figure 4) and, within experimental uncertainty, is independent of dopant and its concentration [9]. The value of $s$ for Ta (0.003) was 2.75 and for Nb (0.003) about 1.4 (see table 2). This latter value compares with 1.6

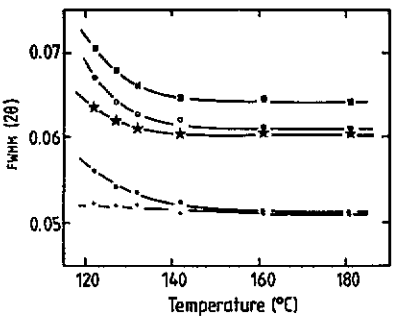


**Figure 3.** Temperature dependence of FWHM of several reflections from Ta (0.003) in the high-temperature phase ($2\theta$ is in degress). Symbols denote: ●, (110); +, (111); ○, (200); *, (211); ■, (220).

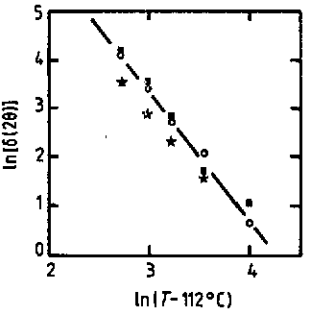


**Figure 4.** Log $[\delta\ (2\theta)]$ against $\log(T - T_s)$ for Ta (0.003) with $T_s$ equal to 112 °C; this value produces a linear plot. The line has a slope of 2.8. Symbols as in figure 3.

**Table 2.** Experimental values for $T_s$ and exponent $s$.

| | $T_s$ (°C) | $s$ |
|---|---|---|
| Impure systems | | |
| Dopants on A-site | | |
| Ce (0.001) | 112 (fixed) | 2.7(3)† |
| Ce (0.003) | 112 (fixed) | 2.8(2)† |
| Dopants on B-site | | |
| Ta (0.003) | 112 (fixed) | 2.8(2) |
| Nb (0.003) | 112 (fixed) | 1.6(2)† |
| Nb (0.003) | 112 (fixed) | 1.4(3) |
| Pure as-purchased material | 112 (fixed) | 1.3(2)† |
| Solid solutions Sr (0.003) | 55(80) | 8(3) |
| Sr (0.010) | 50(80) | 7(3) |
| Sr (0.100) | 20(40) | 4(2) |

† From [9]. All other entries, this work.

determined earlier [9]. The same Nb (0.003) sample was used in both runs. Other impurities produce values around 2.7, and this was why the Nb-doped material was re-examined. The significance of the value of $s$ is discussed in section 5.

The reciprocal dielectric susceptibility in the high-temperature phase of nominally pure $BaTiO_3$ extrapolates to zero at a temperature $T_c$, which is about 13 °C less than the temperature at which the discontinuous change to the ferroelectric form occurs [14], so it is tempting to identify $T_s$ with $T_c$. Since $T_t > T_s$, the transitions are discontinuous.

*4.1.2. $(Ba_{0.997}Sm_{0.003})TiO_3$ [Sm (0.003)].* For Sm (0.003) the fits at elevated temperature using a single peak were poor, with a significant deviation in the tails of the profiles (figure 5). The fit was greatly improved by using two peaks for the calculated profile; the reliability index

$$\left(\sum[I(\text{obs}) - I(\text{calc})]^2 \Big/ \sum I(\text{obs})^2\right)^{1/2}$$

improved from typically 10% to less than 2%. The least-squares fit gave one component a FWHM of 0.05° ($2\theta$), the other about 0.2 ($2\theta$). The need for two peaks suggests that the distribution of dopant is inhomogeneous, with regions rich in samarium. Assuming the width of the broader line at the highest temperatures results from the small size of the dopant-rich clusters, then their effective diameter is about 400 Å or 100 unit cells.

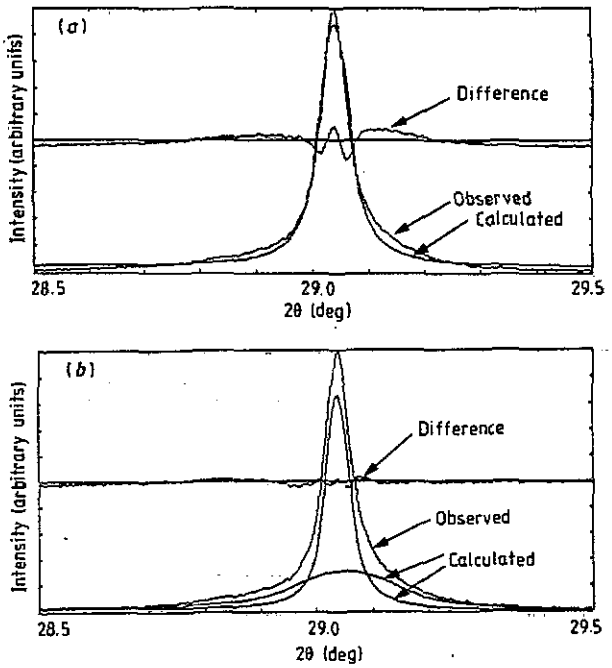


**Figure 5.** Fits to the (200) reflection from Sm (0.003) at 157 °C: (*a*), a single pseudoVoigt; (*b*), two independent pseudoVoigt functions.

Both components increase in width as $T_t$ is approached from above (figure 6). A very rough estimate of the exponent $s$, using three points only for each component, and for this reason not included in table 2, gave 2.4(6).

The ratio of the integrated intensities is also shown in figure 6. It decreases from near unity close to $T_t$ to about 0.5 at higher tempertures. It was argued in [9] that the impurities are 'soft', that is that their presence causes the appearance of the low-temperature structure above $T_t$ of the pure material. The increase in the intensity ratio as temperature is lowered towards $T_t$ reflects the increase in correlation length of order parameter around the defects. Clearly the clustered impurities produce a significant distortion of the structure even at elevated temperatures.

### *4.2. Solid solutions*

*4.2.1.* $(Ba_{0.997}Sr_{0.003})TiO_3$ *[Sr(0.003)],* $(Ba_{0.99}Sr_{0.01})TiO_3$ *[Sr(0.010)] and* $(Ba_{0.9}Sr_{0.1})TiO_3$ *[Sr(0.100)].* The temperature dependence of the FWHM of several reflections from a Sr (0.010) in the high-temperature phase is shown in figure 7. The location of $T_t$ was imprecise, since the peaks were relatively broad at elevated temperature because the level of doping caused a large isotropic strain broadening. The

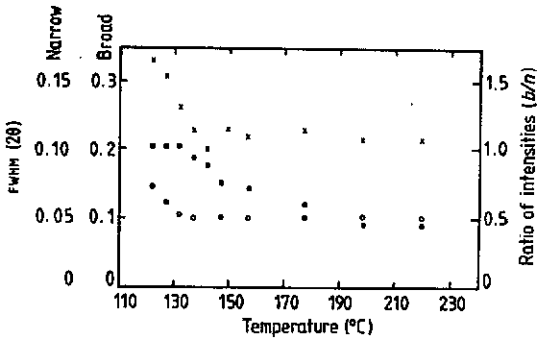


**Figure 6.** Temperature dependence of FWHM for the two components of the (200) reflection from Sm (0.003); ×, broad; ○, narrow. Also plotted (■) is the ratio of their integrated intensities, showing that the broader component becomes weaker at higher temperatures. $2\theta$ is in degrees.

magnitude of the diverging component increased with increasing strontium content very roughly in the ratio 1:2:3 for the three samples; at 10% doping the impurity centres will not behave independently. Analysis of the divergent part of the lines for the three samples produced values for $T_s$ that depend on strontium content. Figure 8 shows the log–log plot of (1) for several values of $T_s$ for the (200) reflection from Sr (0.010). Because $T_t - T_s$ is so large, $T_s$ cannot be determined accurately; values obtained from least-squares fits are included in table 2 along with values for the exponent $s$. Correlation coefficients in excess of 0.99 between the three constants, $W$, $T_s$ and $s$ cause the standard deviations to be large.

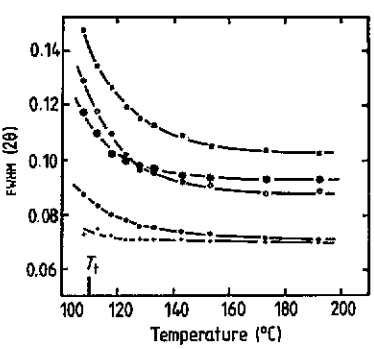


**Figure 7.** Temperature dependence of FWHM of several reflections from Sr (0.010) ($2\theta$ is in degrees). Symbols denote the following reflections: ●, (110); +, (111); ○, (200); *, (211); ■, (220).

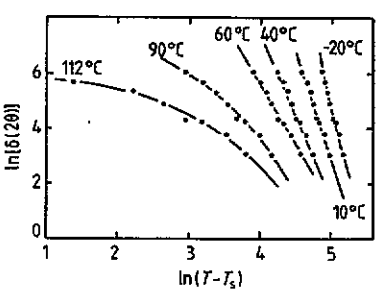


**Figure 8.** Log[$\delta$ ($2\theta$)] plotted against log($T - T_s$) for the (200) reflection from Sr (0.010) for several values of $T_s$. The data are barely sufficient to determine $T_s$, and hence the exponent $s$, since the accessible values of $T$, greater than $T_t$, are much greater than the value of $T_s$, which gives a straight line ($2\theta$ is in degrees).

These materials do not behave as 'host' (pure $BaTiO_3$) plus impurity; the 'host' has been changed by the strontium. In fact, since (Ba, Sr)$TiO_3$ forms a solid solution for all compositions, the notion of strontium being an impurity is inappropriate. Nevertheless, for the compositions studied, the transitions appear to be qualitatively

similar to those in impure systems, that is they are fluctuation-swamped discontinuous changes.

*4.2.2.* $(Ba_{0.99}Pb_{0.01})TiO_3$ *[Pb (0.010)].* The fits at elevated temperatures to the (200) reflection for the lead-doped sample were poor, and as with Sm (0.003), much improved by using two symmetric peaks. Typical FWHM were 0.05 and 0.16° ($2\theta$).

The plot of the angle of maximum intensity of the two components against temperature shows evidence of a discontinuity at 134 °C; figure 9(*a*). Below 134 °C the sample exhibits tetragonal symmetry. The intensity of the broader component is approximately half that of the narrower peak, suggesting that the broader component has the indices (002) and the narrower component is the superimposed doublet (200)/(020). The (002) reflection is the broader peak since the magnitude of $Q_{11}$ is twice that of $Q_{12}$ and the polarization has a relatively large variance.

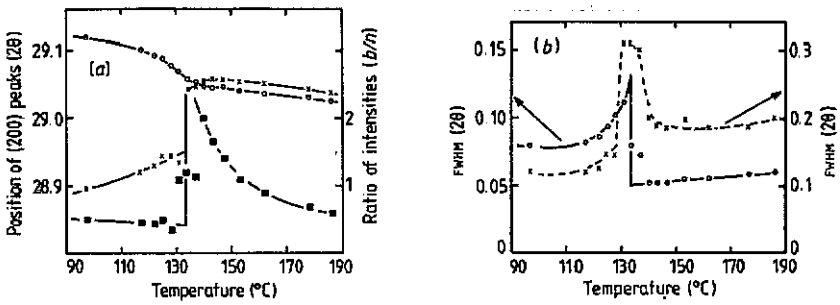


**Figure 9.** (*a*) Temperature dependence of the angles of maximum intensity of the two components of the (200) reflection from Pb (0.010), and the ratio of their integrated intensities, showing that the broader component becomes weaker as temperature increases: ×, broad; ○, narrow; ■, intensity ratio. (*b*) Temperature dependence of the FWHM of two components of the (200) reflection from Pb (0.010): ○, broad; ×, narrow. The lines are visual guides, and $2\theta$ is in degrees.

Above 134 °C the material appears to have two phases, like the samarium-doped sample, with each phase possessing cubic symmetry. The intensity ratio—broad/narrow—decreases with increasing temperature. This suggests that the broader component is produced by polarized clusters that are rich in lead; the increase in intensity ratio with falling temperature is the result of an increase in correlation length as the transition is approached from above. The widths of both components show a rather sharp maximum at about 134 °C (figure 9(*b*)), indicating large polarization fluctuations at the transition. A value for the exponent $s$ could not be determined.

No anomaly in position or width of either component was detected at 490 °C, the transition temperature in pure $PbTiO_3$.

## 5. Discussion

All dopants cause an increase in the spatial variation in the electric polarization in both the high- and low-temperature phases. An excellent discussion of the spatial correlation of the polarization fluctuations in ferroelectrics can be found in the book by Blinc and Zeks, chapter 2 [15]. In an idealized, isotropic system, the leading terms in the free-energy density for $T > T_t$ are

$$g[P(r), T] = g_0(T) + \tfrac{1}{2}a(T - T_c)P^2(r) + \tfrac{1}{2}C(T)[\text{grad } P(r)]^2 \ldots$$

with $C(T) > 0$, and only weakly temperature dependent. Expanding $P(r)$ into a Fourier series

$$P(r) = \sum_q P_q \exp(iq \cdot r)$$

results in the following expression for the mean square fluctuation:

$$\langle |P_q| \rangle^2 = k_B T / a(T - T_c)(1 + q^2 r_c^2)$$

with $r_c$, the correlation length, given by

$$r_c^2 = C(T)/a(T - T_c).$$

More generally, the temperature dependence of the correlation length is of the form

$$r_c \sim (T - T_c)^{-\nu}$$

Values for $\nu$ for various models are listed in table 3.

**Table 3.** Calculated values for $\nu$, $T > T_t$.

| | |
|---|---|
| Exactly soluble models† | |
| Classical | 0.5 |
| Ising model $d = 2$ | 1 |
| Spherical model $d = 3$ | 1 |
| Renormalization group calculations | |
| Isotropic $d = 3$‡§ | |
| Short-range | 0.688 |
| Dipolar | 0.692 |
| Short-range $d = 3$‡ | |
| Ising | 0.638 |
| Planar | 0.675 |
| Heisenberg | 0.7 |

† From [16].
‡ From [21].
§ From [22].

The static pair correlation function,

$$G(r, r') = \langle [P(r) - \langle P \rangle][P(r') - \langle P \rangle] \rangle$$

is obtained from the Fourier transform of $\langle |P_q| \rangle^2$, namely

$$G(r, r') = \langle P(r)^2 \rangle \exp[-|r - r'|/r_c]/|r - r'|$$

which is the Ornstein–Zernike result [16].

The scattered intensity $S(Q)$ is the Fourier transform of $G(R)$ $(R = r - r')$

$$S(Q) = \int_V G(R) \exp(-iQ \cdot R)\, d^3R.$$

To determine $S(Q)$ for an x-ray scattering experiment performed on a crystalline material, the periodic nature of the sample must be considered explicitly. Values of $R$ must equal a real-space lattice vector, that is $R = n_1a + n_2b + n_3c$. At a Bragg reflection, with $Q$ equal to a reciprocal lattice vector $H$, $S(H)$ becomes the volume integral of $G(R)$, and gives the critical part of the scattering; divided by $k_BT$ it is proportional to the ionic contribution to the static dielectric susceptibility. The scattering from the average cubic structure convoluted with the resolution function of the instrument, which has not been considered here, produces the non-critical component of each line.

Defects may be essentially point-like, linear or planar. For point-like defects integration of $G(R)$ must be carried out over three dimensions, and for linear and planar defects in two and one dimensions, respectively. Fisher [17] gives the asymptotic form for $G(R)$ for large $R$ in $d$-dimensions:

$$G(R) \sim \exp(-R/r_c)/R^{(d-1)/2}.$$

The expected dependency of $S(H)$ on $r_c$ for the three cases is summarized in table 4. Since strain couples to the square of the polarization, one would anticipate values of $s$ to equal $2\nu$, $3\nu$ and $4\nu$ for planar, linear and point-like defects, respectively.

**Table 4.** Expected dependence of $s$ on dimensionality of defect.

| Defect type | Planar | Linear | Point |
|---|---|---|---|
| Expected dependence of $S(H)$ on $r_c$ | $r_c$ | $r_c^{3/2}$ | $r_c^2$ |
| Expected value of critical exponent $s$ | $2\nu$ | $3\nu$ | $4\nu$ |

Three of the samples of impure $BaTiO_3$ have values for $s$ around 2.8, close to that expected for point-like defects and short-range interactions. The niobium-doped sample, prepared by the same route as the others and examined on two separate visits to the synchrotron, is the exception; its value of the exponent $s$ is about 1.5.

Godefroy and Levanyuk [18] used Landau theory to estimate the change in transition temperature caused by point defects. They found the reduction in $T_t$ to be proportional to $1 - \eta_0/\eta_\infty$, where $\eta_0$ and $\eta_\infty$ are the magnitudes of the order parameter at the defect core and far from it, respectively. Measurements of permittivity, reported in [8], found little change in $T_t$ for niobium-doped $BaTiO_3$—in contrast to the results reported here. $T_t$ was set equal to the temperature of the maximum in the permittivity. It was concluded in [8] that $\eta_0 = \eta_\infty$, thus making Ba(Ti, Nb)$O_3$ different from the other doped materials they studied. This equality does not imply an infinite correlation length, but rather that the niobium impurities produce virtually no distortion of the structure; as stated in [8], 'the niobium follows titanium in the ferroelectric phase'. In this case the appropriate model would be the random-bond model rather than the random-field model; the latter being more suitable for situations in which impurities cause a local distortion of the structure.

Imry and Wortis [19] find that random fields smear out a discontinuous transition, while Lawrie *et al* [20] conclude that random bonds do not affect the character of the transition.

The as-purchased pure sample shows an interesting type of behaviour, with a broadened transition and significant, spatially varying polarization existing above $T_t$ [9]. The material is severely mechanically strained at room temperature (figure 1), with a large variation in $c/a$ ratio and hence polarization. Presumably the sample has a high density of dislocations. Heating to high temperatures, at least 1200 °C, is required for effective annealing, so the dislocation density during the x-ray experiment will be constant. The crystal has a spatially varying polarization above 130 °C induced through coupling to inhomogeneous strain caused by stress surrounding the dislocations. The random nature of the array of dislocations will favour the presence of many 90° domain walls. These walls are essentially planar, and planar defects produce a value for the exponent $s$ of $2\nu$, that is about 1.4, close to the experimentally determined value.

## 6. Conclusions

Our analysis indicates that none of the impurities introduced change the order of the transition—it is still first order or discontinuous for the level of doping used here—but that fluctuations in the magnitude of the order parameter smother the discontinuity, making the change appear continuous. Fluctuations in the niobium-doped material appear to be different from fluctuations in the other materials we studied. The behaviour in all 'impure' systems, apart from the niobium sample, is that of host plus point-like impurity.

Solid solutions behave differently. The cations introduced are isovalent with the barium that they replace, and so, unlike the 'impure' systems, are not extrinsic semiconductors [10]; the cations introduced are neither charged or screened. The addition of strontium increases the anharmonic contribution to the effective force constant, since $T_s(T_c)$ is depressed [15], and the transition temperature $T_t$ is also lowered. The fluctuations in order parameter are larger the greater the strontium content (figure 2), as one would expect [7].

## Acknowledgment

We wish to thank the UK SERC for funding this research.

## References

[1] Müller K A and Berlinger W 1986 *Phys. Rev.* B **34** 6130
[2] Fontana M D, Bouziane E and Kugel G E 1990 *J. Phys.: Condens. Matter* **2** 8681
[3] Vogt H 1991 *J. Phys.: Condens. Matter* **3** 3697
[4] Cox U J, Gibaud A and Cowler R A 1988 *Phys. Rev. Lett.* **61** 982
[5] Cox U J 1989 *J. Phys.: Condens. Matter* **1** 3565
[6] Cox U J and Cussen L D 1989 *J. Phys.: Condens. Matter* **1** 3579
[7] Bruce A D and Cowley R A 1981 *Structural Phase Transitions* (London: Taylor and Francis)
[8] Godefroy G, Jannot B and Michel-Calendini F M 1991 *Phase Transitions* **33** 3
[9] Darlington C N W and Cernik R J 1991 *J. Phys.: Condens. Matter* **3** 4555
[10] Heywang W 1957 *J. Mater. Sci.* **6** 1214
[11] Burns G 1974 *Phys. Rev.* B **10** 1951
[12] Johnson Matthey plc 1991 private communication

[13] Lines M E and Glass A M 1977 *Principles and Applications of Ferroelectrics and Related Materials* (Oxford: Clarendon)
[14] Burfoot J C 1967 *Ferroelectrics: and Introduction to the Physical Principles* (London: van Nostrand)
[15] Blinc R and Zeks B 1974 *Soft Modes in Ferroelectrics and Antiferroelectrics* (Amsterdam: North-Holland)
[16] Stanley H E 1971 *Introduction to Phase Transitions and Critical Phenomena* (Oxford: Clarendon)
[17] Fisher M E 1962 *Physica* **28** 172
[18] Godefroy G and Levanyuk A 1984 *Ferroelectrics* **54** 301
[19] Imry I and Wortis N 1979 *Phys. Rev.* B **19** 3580
[20] Lawrie I D, Millev Y T and Uzunov D I 1987 *J. Phys. A* **20** 1599
[21] Aharony A and Fisher M E 1973 *Phys. Rev.* B **8** 3323
[22] Bruce A D and Aharony A 1974 *Phys. Rev.* B **10** 2078